SUPPLEMENTAL MATERIAL

Table S1. Sequences of Real-time PCR primers.

Target gene	Accession number	Forward Primers (5 -3')	Reverse Primers (5 -3')
ABCA1	NM_013454	TCCTCATCCTCGTCATTCAAA	GGACTTGGTAGGACGGAACCT
ABCG1	NM_009593	TCACCCAGTTCTGCATCCTCTT	GCAGATGTGTCAGGACCGAGT
ABCG5	NM_031884	TGGATCCAACACCTCTATGCTAAA	GGCAGGTTTTCTCGATGAACTG
ABCG8	NM_026180	TGCCCACCTTCCACATGTC	ATGAAGCCGGCAGTAAGGTAGA
Arg-1	NM_007482	TGGCTTGCGAGACGTAGAC	GCTCAGGTGAATCGGCCTTTT
CD36	NM_001159558	GGAACTGTGGGCTCATTGC	CATGAGAATGCCTCCAAACAC
COX-2	NM_011198	TGCTGTACAAGCAGTGGCAA	GCAGCCATTTCCTTCTCTCC
Cyclophilin	NM_011149	GGAGATGGCACAGGAGGAA	GCCCGTAGTGCTTCAGCTT
HMGCoAR	NM_008255	CCGAATTGTATGTGGCACTG	GGTGCACGTTCCTTGAAGAT
HMGCoAS	NM_008256	GGTGGATGGGAAGCTGTCTA	ACATCATCGAGGGTGAAAGG
ICAM-1	NM_010493	AACCGCCAGAGAAAGATCAG	TGTGACAGCCAGAGGAAGTG
IL-6	NM_031168	GAGGATACCACTCCCAACAGACC	AAGTGCATCATCGTTGTTCATACA
LDLR	NM_001252659	TCCAATCAATTCAGCTGTGG	GAGCCATCTAGGCAATCTCG
Mrc-1	NM_008625	ATGCCAAGTGGGAAAATCTG	TGTAGCAGTGGCCTGCATAG
NF-κB	NM_008689	GAACGATAACCTTTGCAGGC	TTTCGATTCCGCTATGTGTG
NPC1L1	NM_207242	TGGACTGGAAGGACCATTTCC	GACAGGTGCCCCGTAGTCA
TGFβ	NM_011577	TTGCTTCAGCTCCACAGAGA	TGGTTGTAGAGGGCAAGGAC
SR-A	NM_031195	CATGAACGAGAGGATGCTGACT	GGAAGGGATGCTGTCATTGAA
VCAM-1	NM_011693	CTTCATCCCCACCATTGAAG	TGAGCAGGTCAGGTTCACAG

Table S2. The basic echocardiography data after DBZ treatment for 10 weeks in each group at ApoE$^{-/-}$ 25 weeks mice.

	Vehicle	**Atorva**	**DBZ 20**	**DBZ 40**
LVID; d (mm)	4.00±0.01	3.86±0.19	4.21±0.41	3.7±0.08
LVID; s (mm)	2.91±0.16	2.77±0.26	3.18±0.43	2.62±0.19
LVPW; d (mm)	0.66±0.01	0.67±0.01	0.67±0.01	0.64±0.03
LVPW; s (mm)	1.01±0.04	1.02±0.02	1.03±0.02	1.01±0.03
LVAW; d (mm)	0.66±0.01	0.67±0.01	0.67±0.01	0.67±0.01
LVAW; s (mm)	1.00±0.03	1.05±0.02	1.04±0.02	1.02±0.03
EF (%)	53.58±3.38	55.08±6.46	49.73±5.26	56.70±5.44
FS (%)	27.38±2.12	28.48±4.21	25.11±3.05	29.37±3.49

All values are means ± SEM (n=9/group), LVID; d, end-diastolic left ventricular internal dimension; LVID; s, end-systolic left ventricular internal dimension; LV mass, left ventricular mass; LVPW; d, end-diastolic left ventricular posterior wall; LVPW; s, end-systolic left ventricular posterior wall; LVAW; d, end-diastolic left ventricular anterior wall; LVAW; s, end-systolic left ventricular anterior wall; EF, ejection fraction; FS, fractional shortening.
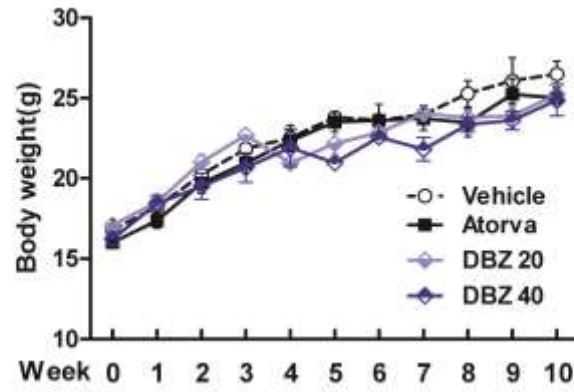
Figure S1. Comparisons of body weight resulting from different treatments in ApoE$^{-/-}$ mice fed a Western diet for 10 weeks. The results are presented as the means $\pm$ SEM (n=9/group). Atorva, atorvastatin.

Figure S2. Representative *in vivo* ultrasound images show the long-axis view of the mouse ascending aorta and innominate artery (IA) in various groups. Peak diastolic flow velocity at the aortic valve (AV, indicated by arrows) was measured and quantified after outlining the Doppler signal. Atorva, atorvastatin.
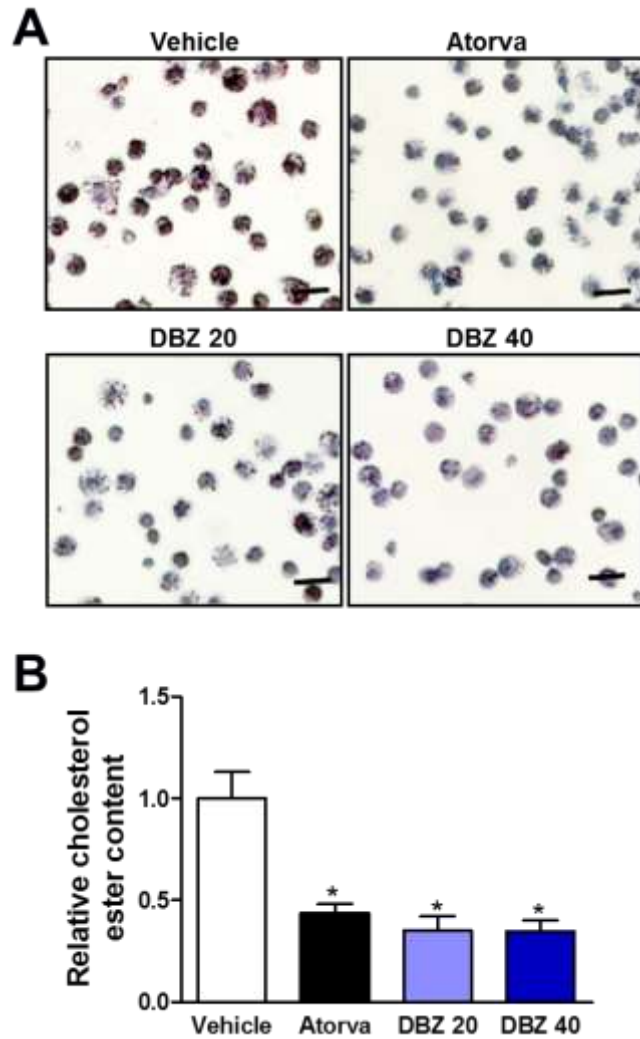
Figure S3. The primary peritoneal macrophages from 25-week-old ApoE$^{-/-}$ mice fed a Western diet for 20 weeks in each group. (A) Cells were cultured for 72 h in complete medium and subsequently stained with Oil Red O (scale: 50 μm). (B) Relative intracellular cholesteryl ester levels were normalized to cellular protein content in peritoneal macrophages. Values are presented as the mean±SEM (n=3/group) (*P<0.05). Atorva, atorvastatin.
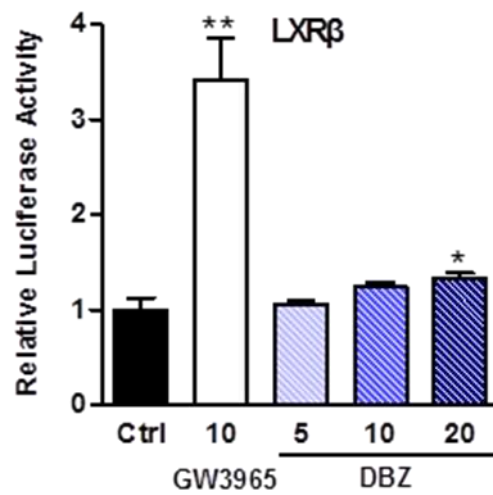
Figure S4. The transcriptional activity of LXRβ was assessed by the transactivation reporter assay in 293T cells. GW3965 was induced as a positive control. Values are presented as the mean ± SEM of at least three experiments (*P<0.05 and **P<0.01). LXRβ, liver X receptor β.
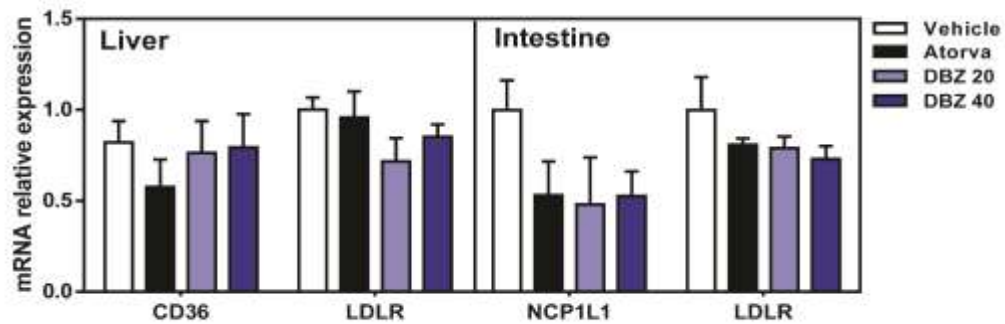
Figure S5. Hepatic and intestinal mRNA levels of genes involved in the transporter of cholesterol as determined by real-time PCR in the mice and normalized to cyclophilin in the mice as indicated in Figure 2 (n=6/group). Atorva, atorvastatin; CD36, cluster of differentiation 36; LDLR, low density lipoprotein receptor; NCP1L1, niemann-pick C 1-like 1.